BBA - Proteins and Proteomics 1866 (2018) 373–378

Contents lists available at ScienceDirect

BBA - Proteins and Proteomics

journal homepage: www.elsevier.com/locate/bbapap

Peroxidase-like activity of cytochrome b_5 is triggered upon hemichrome formation in alkaline pH

Alejandro K. Samhan-Arias[a,*], Luisa B. Maia[a], Cristina M. Cordas[a], Isabel Moura[a], Carlos Gutierrez-Merino[b], José J.G. Moura[a,*]

[a] UCIBIO, REQUIMTE, Departamento de Quimica, Faculdade de Ciências e Tecnologia, Universidade Nova de Lisboa, 2829-516 Caparica, Portugal
[b] Department of Biochemistry and Molecular Biology, Faculty of Sciences, University of Extremadura, 06006, Badajoz, Spain

ARTICLE INFO

Keywords:
Hemichromes
Peroxidase
Low spin state
Hydrogen peroxide
Alkaline pH
Cytochrome b_5

ABSTRACT

In alkaline media (pH 12) a catalytic peroxidase activity of cytochrome b_5 was found associated to a different conformational state. Upon incubation at this pH, cytochrome b_5 electronic absorption spectrum was altered, with disappearance of characteristic bands of cytochrome b_5 at pH 7.0. The appearance of new electronic absorption bands and EPR measurements support the formation of a cytochrome b_5 class B hemichrome with an acquired ability to bind polar ligands. This hemichrome is characterized by a negative formal redox potential and the same folding properties than cytochrome b_5 at pH 7. The acquired peroxidase-like activity of cytochrome b_5 found at pH 12, driven by a hemichrome formation, suggests a role of this protein in peroxidation products propagation.

1. Introduction

Heme protein autoxidation processes are associated *in vivo* to many factors (such as, globin matrix, pH, oxygen pressure and denaturant agents) [1,2]. Hemichromes originate in oxidized heme proteins and present a distorted iron coordination site [3,4]. Although these complexes have been associated to protein denaturation, hemichromes are distinguishable from those generated by denaturation leading to precipitation [5] and loss of the heme [6]. Indeed, a fraction of these complexes is present in the normal heme protein blood population being related to blood diseases [2,7,8,9]. Moreover, in some cases hemichromes have been linked to formation of peroxidation products [10,11]. The most studied protein forming hemichromes upon oxidation is hemoglobin [2,12]. In some of the hemichrome complexes, accessibility of exogenous ligands like water may occur by rearrangement of distal histidines with iron in the heme plane facilitating the access to the heme pocket [2,4,12]. Therefore a role of distal histidines in suiting the barrier for exogenous ligands coordination to the heme has been suggested [2].

Substrate accessibility is crucial for an efficient enzymatic catalysis. In metalloproteins, ligand accessibility is associated to alteration of the coordination properties, sometimes involving conformational changes [8]. In this way, peroxidase activity gained by some hemeproteins depends upon a change on the heme coordination state that allows the interaction with peroxides. An interaction of small anions, promoting or inhibiting peroxidase activity in these enzymes has also been described [9,10].

Cytochrome b_5 (Cb_5) enzymatic properties have been overlooked since the labile not covalently heme bond present in the protein has an inherent inefficiency to interact with substrates, due to a full coordination sphere. However, Cb_5 mutants in the coordinating histidines are capable to form complexes with oxygen [13,14] and CO [15] and a peroxidase-like activity associated to adoption of a non-native state conformation has been reported for an artificial designed *c*-type Cb_5 mutant, with the heme covalently bound to the protein matrix but keeping the coordinating histidines intact [16].

Under alkaline conditions, catalytic activities of metallocompounds have been detected [17–19]. This support that alkaline media is an alternative condition to generate novel reactive species in order to study catalytic reactions mediated in metalloproteins [20,21]. In this communication, we report the acquisition of a peroxidase-like activity by human soluble Cb_5 driven by a hemichrome formation at alkaline pH. Under these conditions, the oxidized form of the protein undergoes a conformational rearrangement allowing hydrogen peroxide to interact with its redox center and triggers this activity.

Abbreviations: CO, Carbon monoxide; Cytochrome b_5, Cb_5; Cyt *c*, Cytochrome *c*; EDTA, Ethylene diamine tetra acetic acid; EPR, Electron paramagnetic resonance; HS, High spin; H_2O_2, hydrogen peroxide; LS, Low spin; LSpH7, pH 7 signal; LSpH12, pH 12 signal; LSpH12′, pH 12 signal′; MPO, Myeloperoxidase; NHE, Normal hydrogen electrode; NO, nitric oxide; NOS, Nitric oxide synthase; OH^-, hydroxide anion; P450, cytochrome P450

* Corresponding authors.
E-mail addresses: alejandro.samhan@fct.unl.pt (A.K. Samhan-Arias), jose.moura@fct.unl.pt (J.J.G. Moura).

http://dx.doi.org/10.1016/j.bbapap.2017.09.010
Received 17 May 2017; Received in revised form 19 September 2017; Accepted 20 September 2017
Available online 27 September 2017
1570-9639/

2. Material and methods

2.1. Purification recombinant human erythrocyte Cb_5

Purification of recombinant human erythrocyte Cb_5 was performed by overexpression of the protein using transformed BL21 (DE3)-derived strains of *E. coli* containing the recombinant plasmid [22]. Briefly, after expression, cells were harvested and disrupted by the use of lysozyme, detergents and protease inhibitors. After precipitation in ammonium sulfate 50%, the lysate was extensively dialyzed against Tris 10 mM, EDTA 1 mM pH 8.1, and loaded in diethylaminoethyl sepharose column (2.5 × 30 cm) previous equilibrated in 10 mM Tris, EDTA 1 mM pH 8.1. A step gradient with increasing concentrations of Tris up to 200 mM was performed in the presence of 0.2% deoxycholate and 0.5% Triton X-100. Cb_5 was eluted from the column using a buffer composed by 10 mM Tris, 1 mM EDTA and 250 mM sodium thiocyanate. A final solution of ammonium sulfate 1.1 M was added to the sample and after mixing, the solution was loaded in a CL sepharose 4B column (2.5 × 10 cm) previously equilibrated in Tris 200 mM, EDTA 1 mM pH 8.1. Cb_5 was eluted without retention. To further purify the protein, the concentrated eluent was loaded in a Sephadex G75 column (2.5 × 50 cm) equilibrated with Tris 150 mM pH 7.5. The sample was concentrated by filtration and glycerol was added before freezing.

2.2. Unfolding measurement

Tryptophan fluorescence of Cb_5 (5 μM) was measured using a fluorescence spectrophotometer (Perkin Elmer 650–40; Perkin Elmer, Norwalk, CT, USA) using quartz thermostated cuvettes (2 ml) at 25 °C. The spectra were recorded using an excitation wavelength of 290 nm. The excitation and emission slits were 2 and 5 nm, respectively. The buffer used in the measurements was potassium phosphate 100 mM, Borate 50 mM, KCl 150 mM, EDTA 1 mM prepared at different pHs, or urea 10 M, under stirring.

2.3. EPR measurements

X-band EPR spectra were recorded using a Bruker EMX 6/1 spectrometer and a dual mode ER4116DM rectangular cavity (Bruker); the samples were cooled with liquid helium in an Oxford Instruments ESR900 continuous-flow cryostat, fitted with a temperature controller. The spectra were acquired at 10 K, with a modulation frequency of 100 kHz, modulation amplitude of 0.5 mT and microwave power of 635 μW. Assays conditions are described in figures captions.

2.4. Electronic absorption measurement

Cb_5 spectra (5 μM) were recorded at 25 °C in buffer: Potassium phosphate 100 mM, Borate 50 mM, KCl 150 mM, EDTA 1 mM at pH 12 using a UV-mini 1240 Shimadzu spectrophotometer.

2.5. Electrochemistry

Cb_5 formal potential was calculated by direct electrochemistry, using cyclic voltammetry (CV); setup: one compartment electrochemical cell, three electrodes configuration, anaerobic conditions (anaerobic chamber). The gold electrode was modified by immersion in a 5% mercaptopropionic acid solution for 30 min in order to promote the formation of a self-assembled layer on the surface. The protein was immobilized on the modified gold working electrode using a cellulose membrane (3.5 kDa cut-off), in a thin-layer configuration. Samples of protein (2.5 mM) were exchanged into potassium phosphate buffer 100 mM, Borate 50 mM, KCl 150 mM, EDTA 1 mM, Neomycin 2.5 mM, used as supporting electrolyte solution being all reagents analytical grade. Blank assays were performed using the modified electrode prepared by the same procedure but without the protein. The experiments were attained using a PGSTAT12 Autolab potentiostat/galvanostat and analysis of the data was performed using GPES (Eco Chimie) software. To obtain the formal potential, blanks were subtracted to the signals obtained in the presence of the protein before calculation. CV assays were performed at different scan rates to define the best conditions (5 mV/s) to measure Cb_5 redox features at the selected pH values. Second scans were used for the analysis. All the potentials were converted and are presented in reference to the normal hydrogen electrode scale (NHE).

2.6. Peroxidase activity measurement

Peroxidase activity of Cb_5 was measured using a fluorimetric method based on the increase of fluorescence induced by Amplex Red (Invitrogen (Carlsbad, CA)) oxidation. The increase of fluorescence was monitored in time using a 2 ml quartz cuvette, after incubation of Cb_5 (20 nM), during 10 min, at 25 °C in potassium phosphate 100 mM, Borate 50 mM, KCl 150 mM, EDTA 1 mM, prepared at pH 12. The fluorescence increment present upon oxidation of Amplex red was measured using a spectrofluorimeter Perkin-Elmer 650–40 with the following set up: excitation and emission wavelengths of 530 nm and 590 nm, with excitation and emission slits of 5 and 10 nm and normal gain. The assay was started by addition of Amplex red and the specific H_2O_2 concentrations indicated in the figure. A calibration curve was prepared with resorufin (the oxidation product of Amplex Red) to calculate the peroxidase activity. The curves for the peroxidase activity dependence upon H_2O_2 and Amplex Red concentration have been fitted to a two substrate Michaelis-Menten kinetic model in accordance with a typical peroxidase cycle expected for Cb_5 at this pH. The data were analyzed with the following equation:

$$v = \frac{[E_0]}{\left(\frac{1}{k_{cat}}\right) + \left(\frac{K_{mA}}{k_{cat}[A]}\right) + \left(\frac{K_{mB}}{k_{cat}[B]}\right)}$$

where v is the initial rate concentration, E the concentration of enzyme, A is the concentration of peroxide, B the reducing agent concentration (in this case Amplex Red) concentration.

3. Results and discussion

We characterized the effect of pH on the electronic absorption spectrum of Cb_5 (Fig. 1). Cb_5 electronic spectra at pH 7.0 (panel a) are characterized by the typical α, β and Soret band of this protein at 558, 528 and 413 nm respectively. Identical spectra were obtained in

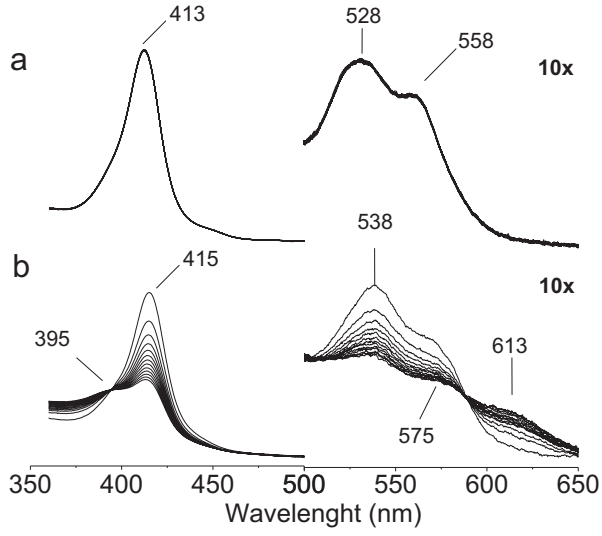

Fig. 1. Cb_5 electronic spectra were recorded at 25 °C every 5 min during 1 h, using a UV-mini 1240 Shimadzu spectrophotometer from 360 to 650 nm in aerobic conditions.

samples prepared from pH 7 to 11 (Supp. Fig. S1). The electronic absorption spectrum of freshly prepared Cb_5 at pH 12 (panel b) shows a displacement of the Soret band from 413 to 415 nm, with shifts in α and β bands to 538 and 575 nm. Cb_5 incubation, during 1 h at pH 12, induced a time dependent disappearance of all bands being the major changes produced after 10–20 min incubation. After this time, bands at 395 and 620 nm also appeared. After changing the pH back from 12 to 7 the characteristic spectra of Cb_5 at pH 7 was recovered suggesting this experiment that the protein changes acquired at pH 12 are reversible (Supp. Fig. S1).

To characterize the coordination properties of the Cb_5 heme at different pH values, we used EPR spectroscopy (Fig. 2A). At pH 7, the Cb_5 EPR spectrum is dominated by a single low spin ($S = 1/2$) Fe^{3+} species, with $g_{1,2} = 3.05$, 2.20 (hereafter designated "pH 7 signal", abbreviated as LS_{pH7}; Fig. 2A, black line). The experimental determination of the g_3 value is difficult (because it occurs at high field and is very broad and weak) and its value was calculated from the Taylor's theorem to be 1.36. These g values ($g_{1,2,3} = 3.05$, 2.20, 1.36) are in agreement with the ones previously described for the pig liver and human erythrocyte Cb_5 ($g_{1,2,3} = 3.03$, 2.23, 1.43, [23] and $g_{1,2,3} = 3.03$, 2.23, 1.39 [24], respectively).

The "Truth Diagram", derived originally by Blumberg and Peisach [25] is useful to predict the heme axial ligands. The "Truth Diagram" correlates the electronic effect of the axial ligands (Δ/λ) with the heme rhombicity (V/Δ) for various heme complexes and provides empirical guidance for the assignment of axial ligands of unknown samples. The "pH 7 signal"-giving species has an axial field strength, $|\Delta/\lambda|$, of 2.73 and a heme rhombicity, $|V/\Delta|$, of 0.86 and, thus, falls in the "B" region on the "Truth Diagram", what is in agreement with the known *bis*-histidinyl coordination of the *b*-type hemes. The EPR spectra of samples prepared from pH 7 to 11 showed an equivalent spectrum.

At pH 12, under aerobic conditions, the EPR spectrum of Cb_5 is dependent on time (Fig. 2A). After 3 min, at pH 12 and room temperature (approximate time needed to freeze the samples), the Cb_5 spectrum shows, besides the "pH 7 signal" (≈ 45%, determined based on the intensity of the g_1 feature), two other low spin ($S = 1/2$) Fe^{3+} species, one with $g_{1,2} = 2.77$, 2.25 and g_3 calculated to be 1.68 and the other with $g_{1,2} = 2.83$, 2.25 and g_3 calculated to be 1.62 (hereafter designated "pH 12 signal" and "pH 12′ signal", respectively; abbreviated as LS_{pH12} and $LS_{pH12'}$, respectively; Fig. 2A, red line). A similar signal was described for the pig liver Cb_5 at pH 12 ($g_{1,2,3} = 2.82$, 2.28, 1.68) [23]. The species giving rise to both LS_{pH12} and $LS_{pH12'}$ (with $|\Delta/\lambda| = 3.80$ and 3.52 and $|V/\Delta| = 0.74$ and 0.75, respectively) falls in "H" region of the "Truth Diagram", as also previously described (for pH 12) [12,25,26], supporting the presence of a *bis*-histidinyl coordinated *b*-type heme. Moreover, the LS_{pH12} signals are similar to the one described for the hemichrome formed during the autoxidation of oxyhemoglobin [12].

After 60 min at pH 12, at room temperature, the proportion of LS_{pH12} + $LS_{pH12'}$ species relatively to the LS_{pH7} increased, but the LS_{pH7} signal did not disappear (Fig. 2A, pink line). In addition to the low spin signals, the Cb_5 EPR spectrum after 60 min at pH 12 displays a very weak axial high spin ($S = 5/2$) signal, with the main component at $g_\perp = 5.8$, for which a $g_{//} \approx 2$ is expected (not resolved here; abbreviated as HS). A similar spectrum was obtained when Cb_5 was incubated at pH 12 and room temperature for 10 min (Fig. 2A, blue line). The presence of a high spin species at high pH had also been described for the pig liver Cb_5 ($g_\perp = 6.2$, pH 12), together with a signal equivalent to our $LS_{pH12}/LS_{pH12'}$ ($g_{1,2,3} = 2.82$, 2.28, 1.68) [23]. The effect of H_2O_2 added to Cb_5 prepared at pH 7 and 12 is shown in Fig. 2B. Left panel shows the EPR spectra of the protein prepared and immediately frozen, at pH 7 in presence of H_2O_2 (10 mM) (black line) in comparison to pH 12 in the presence of H_2O_2 (red line). H_2O_2 addition to samples at pH 12 induced a prominent sharp peak (Δpp = 1.1 mT) centered at g = 2.005 (zoomed EPR spectra shown in the right panel), that correlates with the presence of organic radical species. Moreover, a decrease of the HS signal (g⊥ = 5.8 related to the axial high spin (S = 5/2) signal) was also observed (left panel, indicated by an arrow). Cb_5 EPR

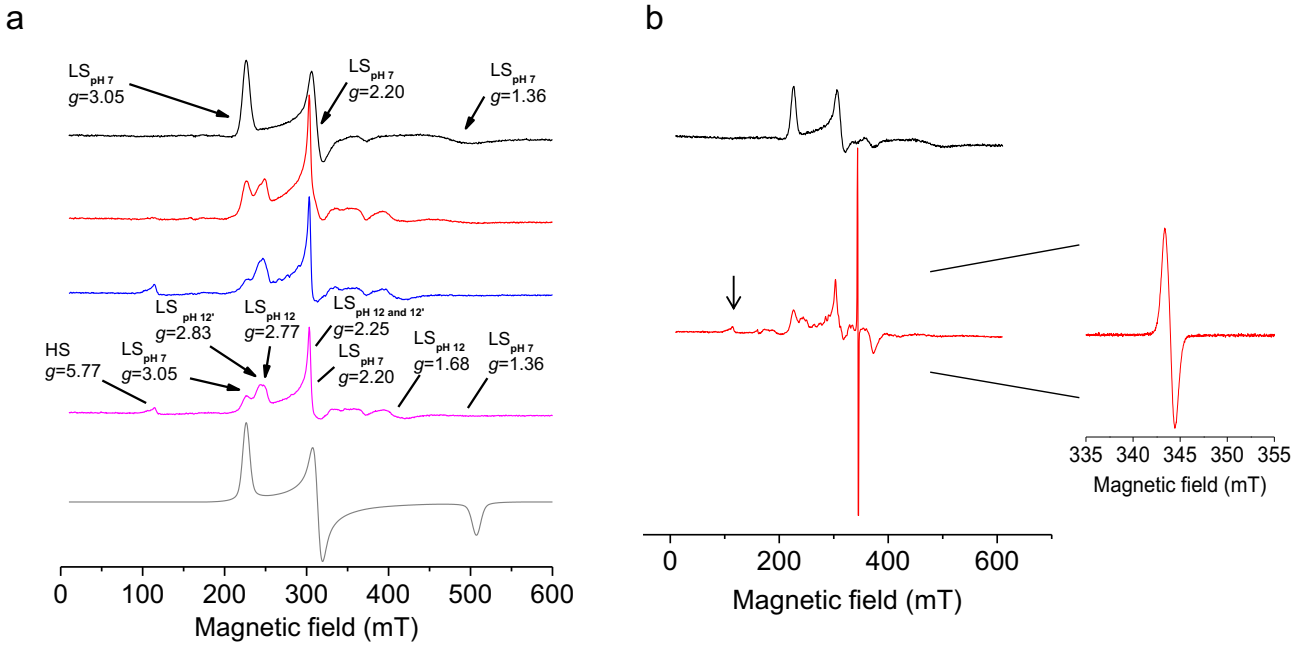

Fig. 2. A. X-band EPR spectra of 2.5 mM Cb_5 at pH 7 and 12. The samples at pH 7 and 12 (black and red lines, respectively) were frozen after 3 min (approximate time needed to freeze the samples). In the case of pH 12, the spectrum was also acquired after the sample being incubated at room temperature for 10 and 60 min (blue and pink lines, respectively). The g values are indicated, as well as, their positions. The simulated spectrum at pH 7 (with $g_{1,2,3} = 3.05$, 2.20, and 1.36) is present in grey. Spectra were recorded at 10 K, with a microwave power of 635 μW and modulation amplitude of 0.5 mT. B. Organic free radical detection by EPR, after H_2O_2 addition to Cb_5 prepared at pH 12. Left panel shows Cb_5 EPR spectra recorded from frozen samples as indicated previously and prepared at pH 7.0 + H_2O_2 (10 mM) (black line) and pH 12.0 + H_2O_2 (10 mM) (red line). Right panel shows the zoomed Cb_5 EPR spectra obtained at pH 12 + H_2O_2 (10 mM) from 335 to 355 mT (magnetic field region) and obtained with the following conditions: temperature 40 K, with a modulation frequency of 100 kHz, modulation amplitude of 0.5 mT and microwave power of 635 μW.

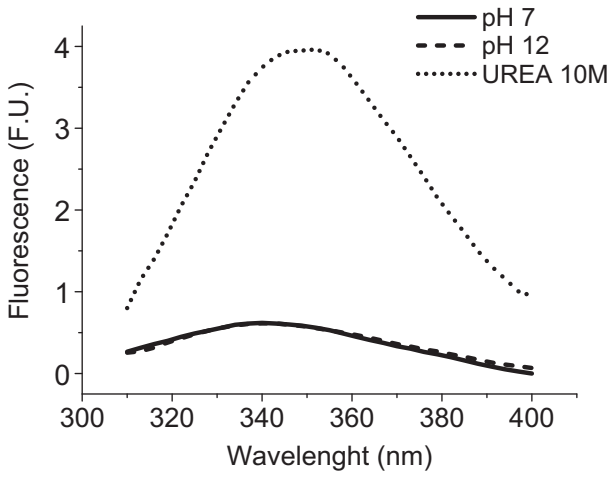

Fig. 3. Maintenance of the native C*b*$_5$ folding state was monitored by measurement of the tryptophan fluorescence intensity. C*b*$_5$ (5 μM) was incubated at pH 7 (continuous line) and 12 (dashed line) during 10 min and its fluorescence was compared to samples prepared in urea 10 M (dotted line) corresponding to the unfolded protein. Fluorescence measurements were performed at 25 °C with excitation wavelength of 290 nm and excitation and emission slits of 2 and 5 nm, respectively.

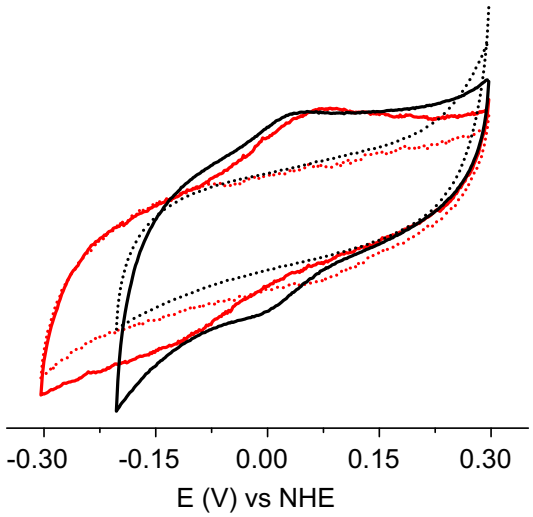

Fig. 4. Cyclic voltammograms of C*b*$_5$ (continuous lines) *vs* its respective controls in the absence of protein (dotted lines), recorded at pH 7 (black lines) and pH 12 (red lines) at 5 mVs^{-1} scan rate, 25 °C. Voltammograms were normalized to the current intensity, for better visualization of the shift in the formal potential.

spectra prepared at pH 7.0, in absence and presence of H_2O_2 shows no significant changes, correlating H_2O_2 interaction dependence with the protein upon the presence of hemichrome species found at pH 12.

C*b*$_5$ maintain a folded state in alkaline buffer (potassium phosphate 100 mM, borate 50 mM, KCl 100 mM, EDTA 1 mM, pH 12) as confirmed by tryptophan fluorescence measurement (Fig. 3). As shown by the effect of 10 M urea, which is known to elicit C*b*$_5$ denaturation [27], C*b*$_5$ unfolding leads to a large increase of the Trp fluorescence intensity like in many other proteins [27,28]. However, the Trp fluorescence intensity of C*b*$_5$ prepared at pH 12 and 7 after 60 min (Supp. Fig. S2) incubation in the buffer was the same and much lower than that measured in the presence of denaturing 10 M urea conditions.

To further characterize C*b*$_5$ properties at pH 12, we observed its electrochemical behavior by cyclic voltammetry and calculated the center formal potential (Fig. 4). A shift of the formal potential from + 13 ± 1 mV at pH 7 (black line) toward − 66 ± 7 mV at pH 12 (red line) was perceived which may be associated to conformational changes, namely a higher solvent exposure [29]. The decrease of reversibility found by the increase of the separation between anodic and cathodic peaks is also in line with such alterations. Lower potentials are usually associated to proteins upon charge, electrostatic and conformational alterations [30,31]. The negative shift of the formal potential of C*b*$_5$ observed at pH 12, is, as so, also consistent with conformational changes in the protein and probably a more exposed heme group.

Reaction of H_2O_2 with C*b*$_5$ prepared at pH 12 and incubated during 10 min, induced a prominent increase of Amplex Red oxidation associated to the presence of protein, being dependent upon H_2O_2 concentration. The interaction of C*b*$_5$ with H_2O_2 upon hemichrome formation is based on the assumption that this peroxidase follows the classical peroxidase cycle where peroxidases (E) consume peroxide and oxidize organic molecules (like Amplex red) to radicals [32]. Therefore the curve obtained for the dependence upon H_2O_2 was fitted to a two substrates Michaelis-Menten equation (Fig. 5). For the H_2O_2 dependence with the peroxidase activity keeping constant protein and Amplex red concentration (AH_2) (0.02 μM and 5 μM, respectively) we obtained the following values: $k_{cat} = 0.7 \pm 0.1\ s^{-1}$, a $K_{m22}^{HO} = 951 \pm 106$ μM and a $K_{m2}^{AH} = 4.2 \pm 0.6$ μM. This equation was also applied for the dependence of Amplex Red with the peroxidase activity of C*b*$_5$, keeping the enzyme and H_2O_2 concentration constant (0.02 μM and 2 mM, respectively) the following kinetic parameter were obtained: a $k_{cat} = 0.8 \pm 0.1\ s^{-1}$, a $K_{m22}^{HO} = 624 \pm 50$ μM and a $K_{m2}^{AH} = 7.2 \pm 0.1$ μM. This activity was independent on the time the protein was incubated at pH 12 and a practical lack of peroxidase activity was found at pHs below 12 (Supp. Fig. S3), showing the strong correlation with the appearance of the hemichrome signal. The measured peroxidase values obtained were higher than those reported for the same activity found in heme proteins of the *b*-type family [33].

In summary, the loss of the electronic spectral properties characteristics of C*b*$_5$ at pH 7.0 supports the hypothesis that the protein

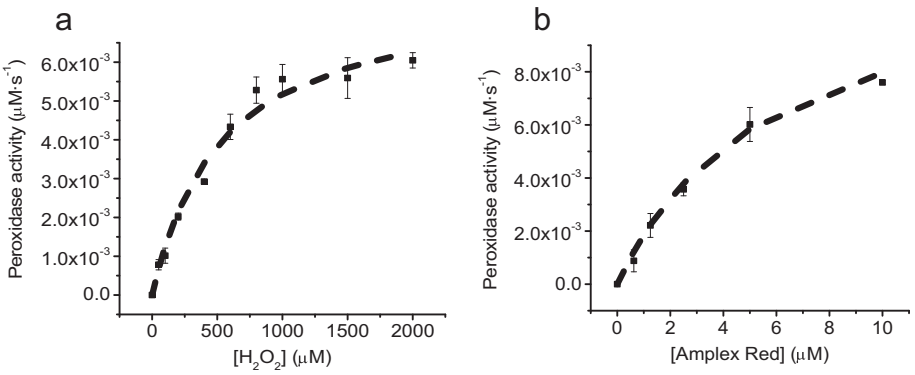

Fig. 5. Initial rates for C*b*$_5$ peroxidase activity dependence upon H_2O_2 were measured with a constant Amplex Red (5 μM) and C*b*$_5$ (20 nM) concentration at pH 12 at 25 °C (panel a). In parallel, initial rates for C*b*$_5$ peroxidase activity dependence upon Amplex Red were measured with a constant H_2O_2 (2 mM) and C*b*$_5$ (20 nM) concentration in buffer at pH 12 at 25 °C (panel b). The kinetic was started after addition of Amplex red or H_2O_2. Averages ± SD of triplicate measurements are shown in the figure and the discontinuous line is the non-linear regression fit to the two substrates Michaelis-Menten model as indicated in Material and Methods.

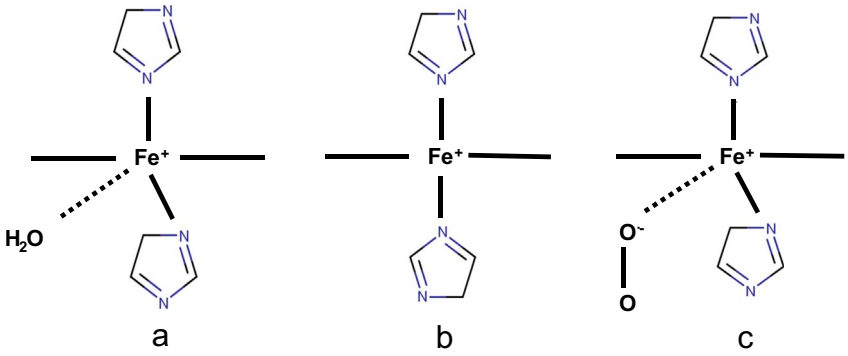

Fig. 6. *Bis*-histidine coordinated hemichromes complexes [2]. Two classes of *bis*-histidine coordinated hemichromes have been documented. Reversible class B (scheme a) with g_1 values around 2.83–2.75, g_3 1.69–1.63 and water present in the ligand pocket (scheme a). Class C (scheme b) with g_1 values around 3.08–2.89, $g_3 \leq 1.51$ with water ejected from the ligand pocket. In some hemeproteins with ability to bind oxygen, superoxide anion has been found to displace oxygen by nucleophilic attack of the distal histidine, being superoxide retained in the ligand pocket (scheme c). In this case, the g values found are similar to the ones or reversible class B hemichrome [4].

itself is a target for oxidation. In addition, appearance of bands at 538 nm, 575 nm and 620 nm has also been found in hemichromes [4,12,34] being reminiscent to that found for compounds III in peroxidases [35]. The lower redox potential of Cb_5 when incubated at pH 12 also supports the tendency to a more oxidized state of the protein at this pH. Moreover, the more negative formal potential value correlates with the values reported for some heme proteins upon interaction with anions, triggering their peroxidase activity, namely, Cyt *c* [36–38] and MPO [39].

The EPR spectra at pH 12 support the formation of a hemichrome. Hemichromes can be classified in different classes depending on the ligand associated to the iron. *Bis*-histidinyl coordinated hemichromes can be categorized in class B, with g_1 values around 2.83–2.75 and g_3 1.69–1.63 with ligand field parameters of reversible hemichrome H and water and or its conjugated ions (OH^- and H^+) retained in the ligand pocket [12]; and class C with g_1 values around 3.08–2.89 and $g_3 \leq 1.51$ with ligand fields falling in the group of irreversible B and C-type hemichromes, with water ejected from the ligand pocket (Fig. 6) [2]. Therefore our LS_{pH12} and $LS_{pH12'}$ species and the electronic absorption bands found are correlative to the reversible type B hemichromes suggesting the opening of an interacting site for polar compounds and/or water [4,12,34] (that at pH 12 would be hydroxyl ion). Similar high spin species to those found in our spectra had also been described in aqua high spin complexes in hemichromes with $g_{\perp} = 5.86$ and $g_{//} \approx 1.99$ [12]. Our EPR data support formation of a radical upon hydrogen peroxide addition that could be attributed to the shorted half-life of compound I. Amplex red oxidation catalysis upon addition of hydrogen peroxide to the buffer in the presence of protein support formation of this type of radical. Formation of an amino acid based radical is needed as the driven factor leading to compound I or II transformation to the resting state in the catalytic cycle of some peroxidases.

In addition, measurement of the folding properties of Cb_5 through tryptophan fluorescence indicates that the protein keeps its folding properties at pH 12, being this non-native state conformation different from those complexes associated to precipitation or loss of the heme [2,5,6].

4. Conclusions

Our experimental results support a peroxidase like activity of human soluble Cb_5 in alkaline conditions upon formation of a hemichrome. The redox potential and the electronic absorbance spectra found for Cb_5 incubated in these conditions are in concordance with the expected for a more oxidized state of the protein. Therefore, the protein has an acquired ability to bind oxygenated species and to be able to catalyze a peroxidase reaction suggesting the opening of ligand site for H_2O_2 as a substrate. The initial steps that promote peroxidase activity are related to low spin signals assigned to class B hemichrome with a reversible acquired accessibility to water like ligands and other polar molecules [4,12,34]. Since hemichromes have been related to formation of peroxidation products [10,11], our results suggest a role of Cb_5 hemichromes in amplification of peroxidase reactions upon its formation.

Supplementary data to this article can be found online at https://doi.org/10.1016/j.bbapap.2017.09.010.

Transparency document

The Transparency document associated with this article can be found, in online version.

Acknowledgment

Recombinant plasmid for human erythrocyte Cb_5 was kindly provided by Dr. A. Grant Mauk from the University of British Columbia, Vancouver, Canada. This work was supported by the Unidade de Ciências Biomoleculares Aplicadas-UCIBIO, which is financed by national funds from FCT/MEC (UID/Multi/04378/2013) and co-financed by the ERDF under the PT2020 Partnership Agreement (POCI-01-0145-FEDER-007728). Experimental work was also partially supported by funding from Ayuda a Grupos de la Junta de Extremadura (GR15139 to Group BBB008) co-financed by the European Funds for Structural Development (FEDER). AKSA and LBM also thank FCT/MCTES for the post-doctoral fellowship grants (SFRH/BPD/100069/2014 and SFRH/BPD/111404/2015, respectively), which are financed by national funds and co-financed by FSE.

References

[1] A. Vergara, L. Vitagliano, C. Verde, G. di Prisco, L. Mazzarella, Spectroscopic and crystallographic characterization of *bis*-histidyl adducts in tetrameric hemoglobins, Methods Enzymol. 436 (2006) (425-425-444).
[2] J.M. Rifkind, O. Abugo, A. Levy, J. Heim, Detection, formation, and relevance of hemichromes and hemochromes, Methods Enzymol. 231 (1994) 449–480.
[3] M. Laberge, K. Szigeti, J. Fidy, The charge transfer band in horseradish peroxidase correlates with heme in-plane distortions induced by calcium removal, Biopolymers 74 (2004) 41–45.
[4] E.A. Rachmilewitz, J. Peisach, W.E. Blumberg, Studies on the stability of oxyhemoglobin A and its constituent chains and their derivatives, J. Biol. Chem. 246 (1971) 3356–3366.
[5] V.W. Macdonald, S. Charache, Drug-induced oxidation and precipitation of hemoglobins A,S and C, Biochim. Biophys. Acta 701 (1982) 39–44.
[6] C.C. Winterbourn, Oxidative denaturation in congenital hemolytic anemias: the unstable hemoglobins, Semin. Hematol. 27 (1990) 41–50.
[7] F. Mannu, P. Arese, M.D. Cappellini, G. Fiorelli, M. Cappadoro, G. Giribaldi, F. Turrini, Role of hemichrome binding to erythrocyte membrane in the generation of band-3 alterations in beta-thalassemia intermedia erythrocytes, Blood 86 (1995) 2014–2020.
[8] K.E. Brown, C.A. Knudsen, Oxidized heme proteins in an animal model of hemochromatosis, Free Radic. Biol. Med. 24 (1998) 239–244.
[9] V.V. Bamm, D.K. Lanthier, E.L. Stephenson, G.S.T. Smith, G. Harauz, In vitro study of the direct effect of extracellular hemoglobin on myelin components, Biochim. Biophys. Acta 1852 (2015) 92–103.
[10] H.J. Andersen, L. Pellett, A.L. Tappel, Hemichrome formation, lipid peroxidation, enzyme inactivation and protein degradation as indexes of oxidative damage in homogenates of chicken kidney and liver, Chem. Biol. Interact. 93 (1994) 155–169.
[11] V.V. Bamm, V.A. Tsemakhovich, N. Shaklai, Oxidation of low-density lipoprotein by hemoglobin-hemichrome, Int. J. Biochem. Cell Biol. 35 (2003) 349–358.

[12] M. Tsuruga, A. Matsuoka, A. Hachimori, Y. Sugawara, K. Shikama, The molecular mechanism of autoxidation for human oxyhemoglobin. Tilting of the distal histidine causes nonequivalent oxidation in the beta chain, J. Biol. Chem. 273 (1998) 8607–8615.
[13] L. Avila, H.W. Huang, C.O. Damaso, S. Lu, P. Moënne-Loccoz, M. Rivera, Coupled oxidation vs heme oxygenation: insights from axial ligand mutants of mitochondrial cytochrome *b*5, J. Am. Chem. Soc. 125 (2003) 4103–4410.
[14] L. Avila, H.W. Huang, J.C. Rodríguez, P. Moënne-Loccoz, M. Rivera, Oxygen activation by axial ligand mutants of mitochondrial cytochrome b_5: oxidation of heme to verdoheme and biliverdin, J. Am. Chem. Soc. 122 (2000) 7618–7619.
[15] Y.W. Lin, J. Wang, Structure and function of heme proteins in non-native states: a mini-review, J. Inorg. Biochem. 129 (2013) 162–171.
[16] S. Hu, B. He, K.-J. Du, X.-J. Wang, S.-Q. Gao, Y.-W. Lin, Peroxidase activity of a c-type cytochrome b_5 in the non-native state is comparable to that of native peroxidases, ChemistryOpen 6 (3) (2017) 325–330.
[17] H.J. Lee, D.L. Lee, C.L. Sedlak, pH-dependent reactivity of oxidants formed by iron and copper-catalyzed decomposition of hydrogen peroxide, Chemosphere 92 (2013) 652–658.
[18] J.B. Wittenberg, Acid and alkaline forms of the higher oxidation state of kangaroo, horse, and sperm whale myoglobin, J. Biol. Chem. 253 (1978) 5694–5695.
[19] S. Tomyn, S.I. Shylin, D. Bykov, V. Ksenofontov, E. Gumienna-Kontecka, V. Bon, I.O. Fritsky, Indefinitely stable iron(IV) cage complexes formed in water by air oxidation, Nat. Commun. 8 (2017) 14099.
[20] T.H. Yosca, J. Rittle, C.M. Krest, E.L. Onderko, A. Silakov, J.C. Calixto, R.K. Behan, M.T. Green, Iron(IV)hydroxide pK(a) and the role of thiolate ligation in C—H bond activation by cytochrome P450, Science 342 (2013) 825–829.
[21] T.H. Yosca, R.K. Behan, C.M. Krest, E.L. Onderko, M.C. Langston, M.T. Green, Setting an upper limit on the myoglobin iron(IV)hydroxide pKa: insight into axial ligand tuning in heme protein catalysis, J. Am. Chem. Soc. 136 (2014) 9124–9131.
[22] E. Lloyd, J.C. Ferrer, W.D. Funk, M.R. Mauk, A.G. Mauk, Recombinant human erythrocyte cytochrome b_5, Biochemistry 33 (1994) 11432–11437.
[23] R. Bois-Poltoratsky, A. Ehrenberg, Magnetic and spectrophotometric investigations of cytochrome b_5, Eur. J. Biochem. 2 (1967) 361–365.
[24] P.G. Passon, D.W. Reed, D.E. Hultquist, Soluble cytochrome b_5 from human erythrocytes, Biochim. Biophys. Acta 275 (1972) 51–61.
[25] W.E. Blumberg, J. Peisach, Probes and Structure and Func-tion of Macromolecules and Membranes, (1971).
[26] A. Levy, P. Kuppusamy, J.M. Rifkind, Multiple heme pocket subconformations of methemoglobin associated with distal histidine interactions, Biochemistry 29 (1990) 9311–9316.
[27] T.E. Huntley, P.J. Strittmatter, The effect of heme binding on the tryptophan residue and the protein conformation of cytochrome b_5, J. Biol. Chem. 247 (1972) 4641–4647.
[28] M.R. Eftink, The use of fluorescence methods to monitor unfolding transitions in proteins, Biophys. J. 66 (1994) 482.
[29] T.C. Santos, A.R. de Oliveira, A.R.J.M. Dantas, C.A. Salgueiro, C.M. Cordas, Thermodynamic and kinetic characterization of PccH, a key protein in microbial electrosynthesis processes in geobacter sulfurreducens, Biochim. Biophys. Acta 1847 (2015) 1113–1118.
[30] T. Aono, Y. Sakamoto, M. Miura, F. Takeuchi, H. Hori, M. Tsubaki, Direct electrochemical analyses of human cytochromes b_5 with a mutated heme pocket showed a good correlation between their midpoint and half wave potentials, J. Biomed. Sci. 17 (2010) 90.
[31] G.R. Moore, G.W. Pettigrew, N.K. Rogers, Factors influencing redox potentials of electron transfer proteins, Proc. Natl. Acad. Sci. U. S. A. 83 (1986) 4998–4999.
[32] F. Nastri, L. Lista, P. Ringhier, R. Vitale, M. Faiella, C. Andreozzi, P. Travascio, O. Maglio, A. Lombardi, V. Pavone, A heme-peptide metalloenzyme mimetic with natural peroxidase-like activity, Chemistry 17 (2011) 4444–4453.
[33] F. Trandafir, D. Hoogewijs, F. Altieri, P. Rivetti di Val Cervo, K. Ramser, S. Van Doorslaer, J.R. Vanfleteren, L. Moens, S. Dewilde, Neuroglobin and cytoglobin as potential enzyme or substrate, Gene 298 (2007) 103–113.
[34] M.S. Navati, J.M. Friedman, Reactivity of Glass-Embedded Met Hemoglobin Derivatives toward External NO: Implications for Nitrite-Mediated Production of Bioactive NO, J. Am. Chem. Soc. 131 (2009) 12273–12279.
[35] B. Valderrama, M. Ayala, R. Vazquez-Duhalt, Suicide inactivation of peroxidases and the challenge of engineering more robust enzymes, Chem. Biol. 9 (2002) 555–565.
[36] L.V. Basova, I.V. Kurnikov, L. Wang, V.B. Ritov, N.A. Belikova, I.I. Vlasova, A.A. Pacheco, D.E. Winnica, J. Peterson, H. Bayir, D.H. Waldeck, V.E. Kagan, Cardiolipin Switch in Mitochondria: Shutting off the Reduction of Cytochrome c and Turning on the Peroxidase Activity, Biochemistry 46 (2007) 3423–3434.
[37] T. Ying, Z.H. Wang, F. Zhong, X. Tan, Z.X. Huang, Distinct mechanisms for the pro-apoptotic conformational transition and alkaline transition in cytochrome c, Chem. Commun. 46 (2010) 3541–3543.
[38] G. Balakrishnan, Y. Hu, T.G. Spiro, His26 protonation in cytochrome *c* triggers microsecond β-sheet formation and heme exposure: implications for apoptosis, J. Am. Chem. Soc. 134 (2012) 19061–19069.
[39] M.J.J. Davies, Myeloperoxidase-derived oxidation: mechanisms of biological damage and its prevention, Clin. Biochem. Nutr. 48 (2011) 8–19.